Journal of
Clinical & Cellular Immunology

Hoozemans et al., J Clin Cell Immunol 2014, 5:4
DOI: 10.4172/2155-9899.1000243

Research Article Open Access

Increased IRAK-4 Kinase Activity in Alzheimer's Disease; IRAK-1/4 Inhibitor I Prevents Pro-inflammatory Cytokine Secretion but not the Uptake of Amyloid Beta by Primary Human Glia

Jeroen J.M. Hoozemans[1*], Elise S. van Haastert[1], Sandra D. Mulder[2], Henrietta M. Nielsen[1,2,4], Robert Veerhuis[2,3], Rob Ruijtenbeek[5], Annemieke J.M. Rozemuller[1], Riet Hilhorst[5], and Saskia M. van der Vies[1]

[1]*Department of Pathology, VU University Medical Center, Amsterdam, The Netherlands*

[2]*Department of Clinical Chemistry, Neurology and Alzheimer Center Amsterdam, VU University Medical Center, Amsterdam, The Netherlands*

[3]*Department of Psychiatry, Neuroscience Campus Amsterdam, VU University Medical Center, Amsterdam, The Netherlands*

[4]*Department of Neuroscience, Mayo Clinic College of Medicine, Jacksonville, Florida 32224, USA*

[5]*PamGene International BV, 's Hertogenbosch, The Netherlands*

[*]**Corresponding author:** Hoozemans JJM, Department of Pathology, VU University Medical Center, P.O. Box 7057, 1007 MB Amsterdam, The Netherlands, Tel: 31-20-4444910; Fax: 31-20-4442964; E-mail: jjm.hoozemans@vumc.nl

Received date: May 11, 2014; **Accepted date:** Jul 29, 2014; **Published date:** Aug 05, 2014

Abstract

Alzheimer's disease (AD) is characterized by the deposition of amyloid-β (Aβ), which is associated with a neuroinflammatory response involving microglia and astrocytes. This neuroinflammatory response has detrimental effects on disease progression but also has a beneficial function on removal of excess Aβ. Microglia and astrocytes are involved in the clearance of Aβ from the brain, but neuroinflammation also promotes neurodegeneration. In order to identify signal transduction pathways critically involved in AD we analysed human brain tissue using protein kinase activity profiling. We identified increased activity of the Interleukin 1 Receptor Associated Kinase 4 (IRAK-4) in AD compared to control brain tissue. IRAK-4 is a component of the signal transduction pathway that functions downstream of the Toll-like receptors and the interleukin-1 receptor. Immunohistochemical analysis of human brain tissue revealed the presence of IRAK-4 in astrocytes and microglia. Quantification of IRAK-4 and the phosphorylated form of IRAK-1, a specific substrate for IRAK-4, revealed increased expression and activity of IRAK-4 in AD. Interestingly, IRAK-1/4 inhibitor I reduces the lipopolysaccharide-induced secretion of monocyte chemotactic protein-1 (MCP-1) by primary human microglia and the interleukin-1β-induced secretion of MCP-1 and interleukin 6 by primary human astrocytes. In contrast, the uptake of Aβ by astrocytes and microglia is not affected by IRAK-1/4 inhibition. Our data show that IRAK-4 protein kinase activity is increased in AD and selective inhibition of IRAK-1/4 inhibits a pro-inflammatory response without affecting the uptake of Aβ by glial cells, indicating that the IRAK signalling pathway is a potential target for modulating neuroinflammation in AD.

Keywords: Alzheimer's disease; Amyloid β; Astrocytes; Interleukin 1 receptor associated kinase 4; Kinase; Microglia; Neuroinflammation

Introduction

Alzheimer's disease (AD) is a chronic neurodegenerative disease and the most common cause of dementia in the elderly. The pathological hallmarks of AD are neuronal loss, amyloid plaques, and neurofibrillary tangles (NFTs). Amyloid plaques primarily consist of amyloid β (Aβ), a cleavage product of the amyloid precursor protein (APP). The build-up of Aβ in amyloid plaques in the brain depends on the balance between Aβ production and the removal or degradation of Aβ. Amyloid plaques in AD brain are closely associated with a local innate immune response marked by activated microglia, reactive astrocytes and the production of proteins that regulate inflammation [1]. The interaction of microglia and astrocytes with Aβ appears to play a dual role in AD pathogenesis. Astrocytes and microglia are important for the removal of excess Aβ from the brain since they can bind and internalize fibrillar as well as oligomeric forms of Aβ [2,3]. However, in an activated state these cells also induce an inflammatory response that has a neurotoxic effect [1,4]. Increased understanding of the underlying processes and signalling pathways that drive the neuroinflammatory response in AD is essential for the development of therapeutic strategies for the treatment of AD.

Cellular pathways, especially those involved in signal transduction to control cell growth, cell division, cellular stress, and inflammation are predominantly regulated by protein kinases. These regulatory enzymes alter the activity of cellular proteins through post-translational modification (phosphorylation). To identify protein kinase activity in post-mortem brain tissue derived from AD and age-matched non-demented control (CTRL) cases we have employed a flow-through peptide microarray system that consists of 140 peptides (13-15 amino acids) derived from known kinase substrate sequences, which have been covalently attached to porous chips [5,6]. Phosphorylation of the peptides by protein kinases and detection of phosphorylated sites was monitored with the use of fluorescently labelled antibodies directed against different phosphorylated epitopes [6,7]. The advantage of this array technology is that the activity of protein kinases is measured, rather than their expression level. Using this technique we found support for an increased activity of Interleukin (IL) 1 Receptor Associated Kinase 4 (IRAK-4) in AD brain tissue. IRAK-4 is a serine/threonine kinase (STK) and a component of the signal transduction pathway that functions downstream of the Toll-like receptors (TLRs) and the IL-1 receptor (IL-1RI) [8]. Upon

ligand binding to either IL-1RI or TLR, the adaptor protein MyD88 binds to the receptor via its so-called TIR domain [9]. Subsequently, IRAK-1 interacts with MyD88, which acts as a scaffold protein onto which IRAK-1 and IRAK-4 assemble [10]. IRAK-4 then phosphorylates IRAK-1 resulting in autophosphorylation and activation of IRAK-1 and the release of IRAK-1 from MyD88 [11]. Binding of IRAK-1 to the adaptor protein tumor necrosis factor (TNF) receptor-associated factor 6 (TRAF6) ultimately leads to NF-κB activation resulting in the production and secretion of pro-inflammatory cytokines [8]. Increased levels of IL-1 are readily detected in microglia associated with early Aβ deposits suggesting an involvement of IL-1 in early AD pathology [12]. In response to IL-1 microglia and astrocytes produce pro-inflammatory cytokines, chemokines, adhesion molecules, prostaglandins, reactive oxygen species, nitric oxide, and matrix metalloproteases [13]. These inflammatory mediators have been implicated in the propagation of AD [1].

TLRs, as well IL-1 and IL-1RI play a key role in the regulation of neuroinflammation during AD. TLRs have a dual role in neuroinflammation since they have been shown to be involved in both the removal of Aβ as well as the increased production of neurotoxic pro-inflammatory molecules in *in vitro* as well as *in vivo* models for AD [14-16]. The significance of TLR signalling in AD has been primarily supported by studies using mouse models for AD that indicate that TLR signalling is important for controlling the levels of Aβ in the brain [17]. Deficiency of the adaptor protein MyD88, which is essential for the downstream signalling of all TLRs (except TLR3) and the interleukin 1 receptor (IL-1RI), resulted in decreased Aβ load and microglial activation [18]. Recently, Cameron and colleagues showed that introducing a kinase inactive form of IL-1 receptor associated kinase 4 (IRAK-4) in an AD mouse model reduced the amyloid burden and gliosis in older animals [19].

In the present study we show that the IRAK signalling pathway is activated in brain tissue derived from AD patients and that inhibition of the IRAK signalling pathway reduces a proinflammatory response without affecting the uptake of Aβ by human glial cells. Our results provide support for the IRAK signalling pathway as a potential target for modulating the inflammatory response in AD.

Materials and Methods

Post-mortem human brain tissue

Post-mortem brain material of AD and age-matched non-demented control cases was obtained from the Netherlands Brain Bank (Amsterdam, The Netherlands). All donors or their next of kin provided written informed consent for brain autopsy and use of tissue and medical records for research purposes. Staging of AD pathology was evaluated according to Braak and Braak [20]. Age, gender, clinical diagnosis, stage of AD pathology (Braak score), and post-mortem delay (PMD) of the cases used in this study are summarized in Table 1.

Cases used for immunohistochemistry					
	N	**Sex (M/F)**	**Average age in years (range)**	**Average Braak stage (range)**	**Average PMD in hours (range)**
CTRL	11	8/3	72 (46-85)	0.4 (0-1)	7 (5-10)
AD	11	6/5	73 (63-93)	5.5 (4-6)	6 (4-9)
Cases used for kinase activity profiling					
	N	**sex (M/F)**	**Average age in years (range)**	**Average Braak stage (range)**	**Average PMD in hours (range)**
CTRL	6	5/1	73 (64-85)	0.3 (0-1)	7 (5-8)
AD	7	5/2	71 (63-85)	5.1 (4-6)	6 (4-9)
CTRL: Control case; AD: Alzheimer's Disease patient; F: Female; M: Male; N: Number of cases; PMD: Post Mortem Delay					

Table 1: Control and AD cases used for generating kinase activity profiles and/or immunohistochemistry.

Serine/threonine kinase activity profiling

Brain tissue samples from the temporal cortex were collected during autopsy, snap frozen and stored in liquid nitrogen. Protein extracts were prepared by lysis of brain tissue in M-PER (Thermo Scientific, Rockford IL, USA) containing protease inhibitors (Complete protease inhibitor cocktail, Roche, Mannheim, Germany) and phosphate inhibitors (PhosSTOP, Roche) for 30 min at 4°C. Total soluble cell lysate was obtained by centrifugation at 12.000 × g for 10 min at 4°C. Protein concentration was determined using the Bio-Rad (Hercules, CA) protein assay with bovine serum albumin (BSA, Boehringer Mannheim, Germany) as standard. Assessment and analysis of protein kinase activity was performed using the PamChip® peptide microarrays (PamGene, Hertogenbosch, The Netherlands) [6]. The sample mixture consisted of 1 × ABL buffer (Westburg, Leusden, The Netherlands), 500 µmol/L ATP (Sigma-Aldrich, St. Louis, MO), 0.1 mg/ml BSA (New England Biolabs, Ipswich, MA) and either 0.5 µg proteins from brain tissue lysate or 0.1 µg human recombinant IRAK-4 (Proqinase, Freiburg, Germany). IRAK-1/4 inhibitor I (Sigma-Aldrich) was used at a concentration of 2.5 µM (stock solution was prepared in dimethylsulfoxide (DMSO) at a concentration of 2.5 mM).

Before loading the reaction mixture, the array was blocked with a 2% (w/v) BSA solution (Calbiochem). Sample mixtures were applied in quintuple and the solution was pumped up and down for 30 cycles (1 cycle/min). After washing three times with PBS containing 0.01% (v/v) Tween 20, detection mix was added consisting of PBS containing 1% (w/v) BSA, rabbit anti-phospho-MAPK Substrates (PXTP) (clone 46G11, dilution 1:100, Cell Signaling Technology, Beverly, MA), rabbit anti-phospho-PKA substrate (RRXS*/T*) (clone 100G7E, dilution 1:250, Cell Signaling Technology), rabbit anti-phospho-MAPK/CDK substrates (PXS*P or S*PXR/K) (clone 34B2, dilution 1:250, Cell Signaling Technology), rabbit anti-phospho-Akt substrate (RXXS*/T*)

(clone 110B7E, dilution 1:250, Cell Signaling Technology), and secondary goat anti-rabbit IgG conjugated to fluorescein isothiocyanate (FITC) (dilution 1:50, Santa Cruz Biotechnology, CA). Detection mix was pumped up and down for 60 cycles (2 cycles/min). After washing, images were captured with a CCD camera using different exposure times. Quantification of FITC intensities was conducted using Bionavigator software (PamGene). Spot intensities of sample without ATP were taken as background. Differences in peptide phosphorylation were statistically assessed using nonparametric Mann-Whitney U tests in SPSS (version 16.0 for Windows, SPSS Inc).

Immunohistochemistry/immunofluorescence

Sections (5 µm thick) of fresh frozen tissue from the mid-temporal cortex were mounted on to Superfrost plus tissue slides (Menzel-Glaser, Germany) and fixed by immersion in acetone (100%) for 10 minutes. Primary antibodies were diluted in phosphate-buffered saline (PBS) containing 1% (w/v) BSA. Sections were incubated O/N with primary antibodies at 4°C (Table 2). Primary antibodies were detected using EnVision (DAKO, Glostrup, Denmark) and color was developed using 3,3'-diaminobenzidine (DAKO). Sections were counterstained with hematoxylin and mounted using Depex (BDH Laboratories Supplies, Poole, England). Negative controls for single immunostainings were generated by omission of primary antibodies. Contiguous microscopic fields arranged in columns were examined with a 10× objective. Full colour images were obtained using a Zeiss light microscope equipped with a digital camera. The area density was quantified using Image-Pro Plus analysis software (Media Cybernetics, Silver Spring, MD). Using this method the percentage of the area of interest i.e. the area of immunoreactivivity for a specific antibody is measured. Assessments for different antibodies were performed in adjacent sections and blind to the pathological and clinical categorization. Student's t-test was used to determine differences between CTRL and AD cases. Results are expressed as mean ± standard deviation (SD). $P<0.05$ was considered significant.

Antibody (antigen)	Species	Dilution	Source
AT8 (Tau pSer202 and pThr205)	mouse	1:1000	Pierce, Rockford, IL, USA
Aβ1-17	mouse	1:50	Dako, Glostrup, Denmark
CD68 (clone KP1)	mouse	1:2400	Dako, Glostrup, Denmark
GFAP	mouse	1:50	Monosan, Uden, The Netherlands
IRAK-4	rabbit	1:200	Sigma-Aldrich, St. Louis, MO
IRAK-4	rabbit	1:100	Cell Signalling, Beverly, MA
IRAK-4	mouse	1:200	Millipore, Billerica, MA
IRAK-1	mouse	1:125	Sigma-Aldrich, St. Louis, MO
pIRAK-1(Ser 376)	rabbit	1:50	Santa Cruz Biotechnology, CA

Table 2: Primary antibodies used in this study.

For double labeling by immunofluorescence, sections were preincubated with 10% (v/v) normal goat serum (DAKO) in PBS for 10 min at RT and with either anti-IRAK-4, anti-GFAP or anti-CD68 O/N at 4°C. For the detection of anti-GFAP and anti-CD68 goat anti-mouse IgG1 conjugated to biotin (Southern Biotechnology Associates, Birmingham, AL) was added (1:100 dilution). After incubation of the sample for 60 min at RT streptavidin Alexa488 (Molecular Probes, Leiden, The Netherlands, (excitation 495 nm, emission 519 nm; green fluorescence)) was added (1:750 dilution) and incubation continued for an additional 60 min at RT. For the detection of anti-IRAK-4, goat anti-rabbit conjugated to HRP (Envision, DAKO) was used (1:100 dilution, 60 min, RT) followed by rhodamine/tyramine intensification (excitation 550 nm, emission 570 nm; red fluorescence). Sections were analyzed using a Leica DMR Confocal LaserScan microscope (Leica, Deerfield, IL). Negative controls for double immunostainings were generated by omitting the primary antibodies.

In vitro functional assays

Adult primary human astrocytes or microglia were isolated from brain specimens obtained at autopsy through the Netherlands Brain Bank and cultured as described earlier [21,22]. Patients gave informed consent, and the use of the tissue for experiments was in compliance with the Declaration of Helsinki and approved by the local Medical Ethics Committee at the VUmc. Primary astrocyte and microglia cultures from different clinically diagnosed AD patients and controls were included in this study.

The human glioblastoma cell line U373 (HTB-17) was obtained from American Type Culture Collection (ATCC, Rockville, MD). Cells were grown (at 37°C; 5% CO_2) as monolayer in culture medium (Dulbecco's modified Eagle's medium (DMEM) and Ham's F10 Nutrient Mixture (Ham-F10) (1:1) supplemented with 10% (v/v) fetal bovine serum (FBS, ICN Biomedicals), 100 IU/ml penicillin and 50 µg/ml streptomycin). Before stimulation/inhibition, U373 cells, primary astrocyte cultures (passage 3-5) and primary microglial cell cultures (passage 0) were trypsinized and transferred to 24-wells plates (Nunc, Roskilde, Denmark) at 5×10^4 cells/well in culture medium. IRAK-1/4 inhibitor I (Sigma) stock solution was prepared in dimethylsulfoxide (DMSO) at a concentration of 2.5 mM. IRAK1/4 inhibitor I as well as vehicle controls (DMSO) were added to the cultures 60 min before incubation with either human recombinant interleukin 1-β (IL-1β) (10 U/ml, Genzyme Diagnostics, Cambridge, MA) or lipopolysaccharide (LPS, 1 µg/ml, E55:B5, Sigma-Aldrich) in culture medium containing 0.1% (v/v) FBS. After 6 or 24 hrs incubation conditioned cell culture medium was collected and stored at -20°C until further analysis for the presence of monocyte chemoattractant protein-1 (MCP-1) and interleukin-6 (IL-6), using the DuoSet MCP-1 enzyme linked immuno-sorbent assay (ELISA)

(R&D Systems Europe, Abingdon, UK), or the Pelipair IL-6 ELISA kit (Sanquin, The Netherlands). To investigate the effect of IRAK-1/4 inhibitor I on cell viability the MTT assay was performed [23]. In short, formazan generated by viable cells by conversion of tetrazolium reagent 3-(4,5-dimethylthiazol-2-yl)-2,5-diphenyltetrazolium bromide (MTT; Sigma) was solubilised in DMSO and the absorbance was determined using a microplate reader at 540 nm. ANOVA followed by Bonferroni's test was used to determine differences between means. Results are expressed as mean ± standard deviation (SD). $P<0.05$ was considered significant.

Aβ1-42 preparations and flow cytometry

Aβ1-42 (Bachem, Weil am Rhein, Germany) was dissolved in hexafluoroisopropanol (Sigma-Aldrich), aliquoted, speed-vacuum dried and stored at -80°C until use, as previously described [24]. Fluorescent (FAM-labelled) Aβ1-42 preparations enriched in oligomers (O-Aβ1-42) and fibrils (F-Aβ1-42) were prepared as described before [25]. Uptake of O-Aβ1-42 and F-Aβ1-42 by microglia and astrocytes was quantified by flow cytometry as described earlier [2,3,24]. In short astrocytes or microglia were plated (2.5×10^4 cells/well) in 24-well plates (Nunc) and allowed to adhere two days prior to experiments. IRAK-1/4 inhibitor I as well as vehicle controls were added to the cells 60 min before incubation with O-Aβ1-42 or F-Aβ1-42. Based on previous results [24], cultures were exposed either to 10 μM O-Aβ1-42 or F-Aβ1-42 for 24 hrs. After treatment with a solution of 0.25% (w/v) trypsin at RT, cells were harvested by centrifugation at 275 × g for 5 min at 4°C, washed in cold FACS buffer (0.25% (w/v) BSA in PBS) and re-suspended in FACS buffer. Aβ-positive cells were quantified using FACS Calibur (BD, Franklin Lakes, NJ) with CellQuest software. Cells were gated based on morphological appearance (forward and side scatter) to count all viable cells and exclude cellular debris and death cells. To ensure that Aβ-uptake was quantified using homogenous cell populations (from individual cultures), the same gates (different for astrocytes and microglia) were used for all experiments. Uptake of Aβ was expressed as percentage of Aβ-positive cells of a total cell count of at least 5.000 counts per condition. In each individual experiment 1% of non-Aβ treated cells were gated as fluorescence-positive, to account for auto-fluorescence, and used as reference upon quantification of Aβ-positive cells. ANOVA followed by Bonferroni's test was used to determine differences between means. Results are expressed as mean ± SD and shown as normalized data (percentage of untreated cells). $P<0.05$ was considered significant.

Results

Serine/threonine kinase profiling on post-mortem human brain tissue

Serine/threonine protein kinase (STK) activity profiles from human temporal cortex specimens were determined by applying protein lysates to the PamChip (STK) either in the absence or the presence of ATP [15]. A clear ATP-dependent profile of phosphorylated peptides was observed, indicative of the presence of STK activity in post-mortem human brain tissue (Figure 1). Data analysis included identification of single peptides showing increased or decreased of ATP-dependent phosphorylation in AD (n=7) compared to CTRL (n=6) cases. Phosphorylation of 11 peptides was found to be significantly increased in AD cases (Table 3). Changes in STK profiles were independent of age, gender or post-mortem delay. The peptides showing a significant increase in phosphorylation between AD and CTRL derived brain tissue were compared with phosphorylation profiles of human recombinant protein kinases generated under similar experimental conditions. Of the peptides differentially phosphorylated between CTRL and AD brain tissue, 4 were found to be significantly phosphorylated by human recombinant IL-1 receptor-associated kinase (IRAK-4) (Table 3). To validate potential phosphorylation of these peptides by IRAK-4, the kinase activity profile of human recombinant IRAK-4 was determined in the presence of IRAK-1/4 inhibitor I [26]. Signal intensities obtained with three out of the four peptides after phosphorylation by recombinant IRAK-4, were reduced by more than 50% in the presence of 2500 nM IRAK-1/4 inhibitor I (Table 3). Together these data support a possible involvement of IRAK-4 in AD and led us to further investigate IRAK-4 in AD brain tissue.

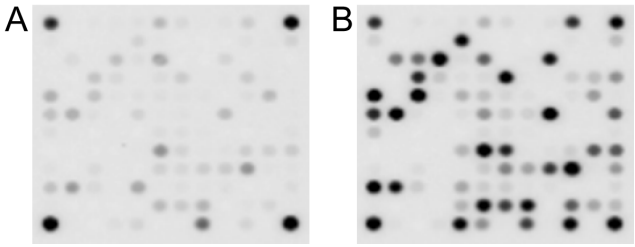

Figure 1: Phosphorylation of peptides on PamChip by protein lysate derived from post-mortem human brain tissue, either **(A)** in the absence of ATP and **(B)** in the presence of 500 μM ATP. Shown are profiles obtained from a representative AD case. The Phosphorylation profile is seen as fluorescent spots (black) on a white background. In each corner a specific phosphorylated peptide is spotted as a reference and internal assay control.

Expression and localization of IRAK-4 and (p)IRAK-1 in CTRL and AD brain

To confirm the involvement of IRAK-4 in AD pathology the presence of IRAK-4, IRAK-1 as well as phosphorylated (p)IRAK-1 was investigated by immunohistochemistry using post-mortem brain tissue derived from AD and CTRL cases. Figure 2 shows representative results from adjacent sections from a CTRL (Braak stage 0) and an AD case (Braak stage 4). No Aβ plaques were detected in CTRL cases while the AD cases showed classical and diffuse Aβ plaques (Figures 2A and 2B). No immunoreactivity for phosphorylated tau (pTau) was observed in the control cases (Figure 2C). The AD cases showed clear presence of pTau in neurites and plaques (Figure 2D). For IRAK-4 three different antibodies were used and all showed identical results regarding the localization and expression in the medial temporal cortex. Based on morphology IRAK-4 immunostaining could be observed in glial cells, primarily astrocytes and microglia, in CTRL brain tissue (Figure 2E). In AD cases a prominent increase in IRAK-4 immunostaining was observed in glial cells (Figure 2F). Active IRAK-4 phosphorylates IRAK-1 resulting in the autophosphorylation and activation of IRAK-1 [13]. IRAK-1 immunostaining could be observed in glial cells, but occasionally also in neurons in CTRL brain tissue (Figure 2G). In AD cases, levels of IRAK-1 immunoreactivity in glial cells showed a modest increase compared to CTRL cases (Figure 2H). Detection of pIRAK-1 showed low levels of immunoreactivity in CTRL cases and was primarily localized in microglia and astrocytes

(Figure 2I). In AD cases pIRAK-1 immunoreactivity was markedly increased and intense immunostaining was observed in microglia and astrocytes (Figure 2J). Quantification of the immunohistochemical signals showed that IRAK-4 and pIRAK-1 expression levels are significantly increased in AD compared with CTRL cases (Figure 3). Levels of IRAK-1 were not significantly different between CTRL and AD cases. The significant increase of pIRAK-1 in AD brain indicates that IRAK-4 kinase activity is increased since IRAK-1 is a specific substrate for IRAK-4. These data support the observed increase in IRAK-4 kinase activity in AD cases as determined by protein kinase activity profiling (Table 3). The cellular localization of IRAK-4 in microglia and astrocytes was confirmed by double immunofluorescence staining. In a representative AD case, IRAK-4 was co-localized with CD68 (Figures 4A-4C) or with GFAP (Figure 4D-4F), indicating that IRAK-4 is present in microglia and astrocytes respectively. Together this data indicates that the IRAK signalling pathway is primarily present in microglia and astrocytes, and that the activity of this signalling pathway is increased in AD compared with CTRL cases.

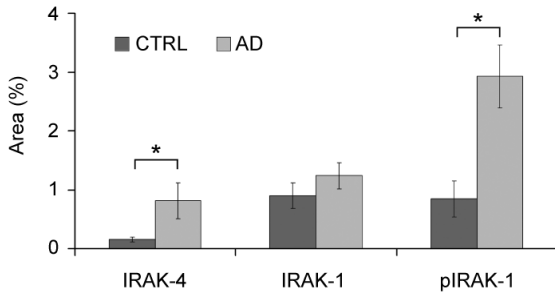

Figure 3: Quantification of IRAK-4, IRAK-1 and pIRAK-1 in CTRL and AD temporal cortex. Mean levels (± SD) of the area density expressed as percentage immunoreactive area of total area for the immunohistochemical staining of IRAK-4, IRAK-1 and pIRAK-1 in CTRL (n=11) and AD (n=11) temporal cortex. * p<0.05.

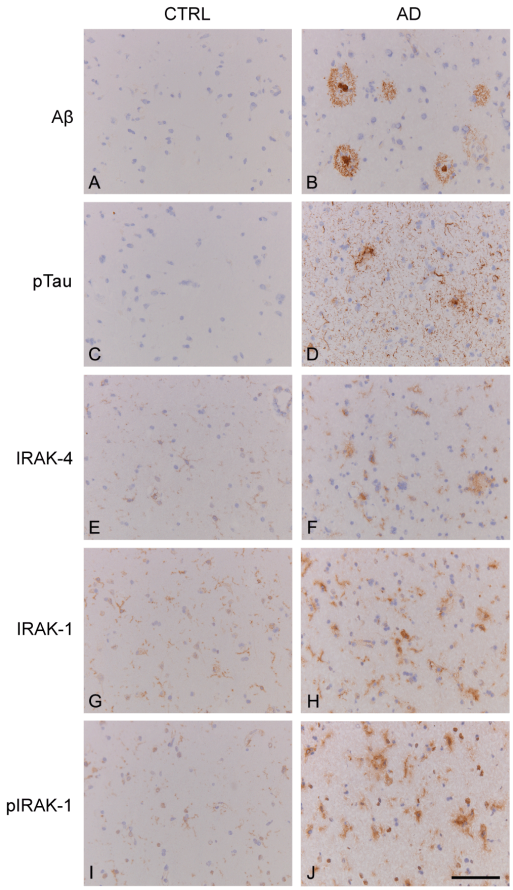

Figure 2: Immunohistochemical detection of IRAK-4, IRAK-1 and pIRAK-1 in CTRL and AD temporal cortex. Shown are immunohistochemical stainings of adjacent sections from a representative CTRL and AD case. Section were stained for Aβ (Aβ1-17) **(A,B)**, pTau (AT8) **(C,D),** IRAK-4 **(E,F),** IRAK-1 **(G,H)** and pIRAK-1 **(I,J)**. Scale bar A-F 100 μm.

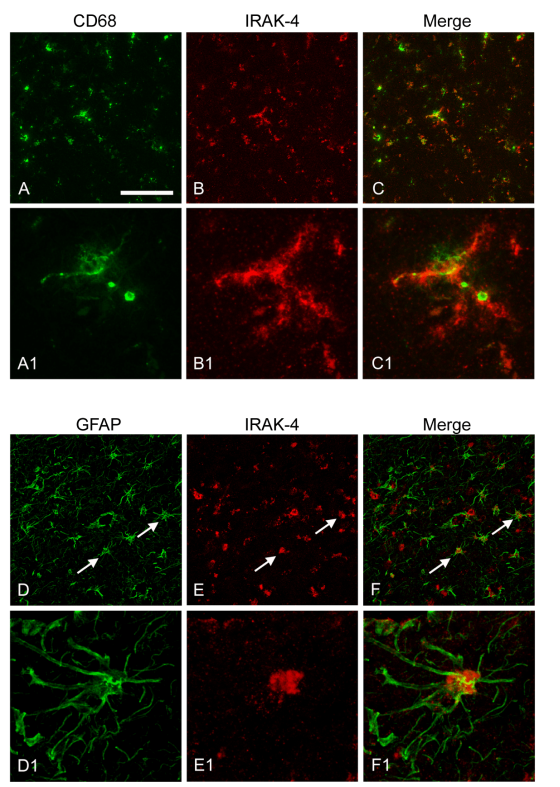

Figure 4: Localization of IRAK-4 in microglia and astrocytes by double-immunofluorescence staining. **(A-C)** Immunofluorescent staining of CD68 (A, green) and IRAK-4 (B, red) in the temporal cortex of a representative AD case (higher magnification depicted in A1-C1). **(D-F)** Double staining for GFAP (D, green) and IRAK-4 (E, red) in the temporal cortex of a representative AD case (arrows indicate double-labelling, higher magnification depicted in D1-F1). Scale bar A-F: 50 μm; scale bar A1-F1: 10 μm

ID	Protein name	UniProt Accession	Sequence	P value
ACM1_421_433	Muscarinic acetylcholine receptor M1	P11229	CNKAFRDTFRLLL	0.046
ACM4_456_468	Muscarinic acetylcholine receptor M4	P08173	CNATFKKTFRHLL	0.015
ACM5_498_510	Muscarinic acetylcholine receptor M5	P08912	CNRTFRKTFKMLL	0.032
ADDB_696_708	Beta-adducin	P35612	GSPSKSPSKKKKK	0.022
CDK7_163_175 * #	Cell division protein kinase 7	P50613	GSPNRAYTHQVVT	0.032
CSK21_355_367	Casein kinase II subunit alpha	P68400	ISSVPTPSPLGPL	0.018
FOXO3_25_37 *	Forkhead box protein O3	O43524	QSRPRSCTWPLQR	0.015
H32_3_18 * #	Histone H3.2	Q71DI3	RTKQTARKSTGGKAPR	0.045
INSR_1368_1380 * #	Insulin receptor precursor	P06213	KKNGRILTLPRSN	0.032
MP2K1_287_299	Dual specificity mitogen-activated protein kinase kinase 1	**Q02750**	PPRPRTPGRPLSS	0.022
P53_308_323	Cellular tumor antigen p53	P04637	LPNNTSSSPQPKKKPL	0.038

* Peptides showing increased phosphorylation by human recombinant IRAK-4 (0.1 µg)

Peptides phosphorylated by human recombinant IRAK-4 (0.1 µg) showing decreased (>50%) phosphorylation in the presence of 2500 nM IRAK-1/4 inhibitor I

Table 3: Peptides on PamChip showing significant increase in phosphorylation by protein lysates derived from AD temporal cortex compared to control temporal cortex. P values indicate significant differences between control and AD cases. Peptides that are potentially phosphorylated by IRAK-4 are shown as indicated.

IRAK-1/4 inhibitor I reduces the pro-inflammatory response in human primary glial cells

Since IRAK-4 is primarily observed in microglia and astrocytes, the effect of IRAK-1/4 inhibitor I (IRAK inh) on the pro-inflammatory response elicited by human primary glial cells in the presence of IL-1β or LPS was studied. Results from the MTT assay indicated that the mitochondrial activity, as a measure for cell viability, was not affected by IRAK inh at concentrations ranging from 250 to 5000 nM. For this study human primary astrocytes and microglia were isolated from brain tissue (mid-temporal lobe) from AD as well as non-AD (non-demented control) cases. No significant differences between AD and non-AD derived glial cells were observed in the *in vitro* functional experiments.

Secretion of MCP-1 and IL-6 by human primary astrocytes was increased when exposed for 24 hrs to 10 U/ml IL-1β (Figure 5A). IRAK inh (range 2500-5000 nM) significantly decreased the IL-1β induced secretion of MCP-1 and IL-6 in a dose-dependent manner. The presence of 2500 nM IRAK inh showed a more than 50% reduction in the IL-1β induced secreted levels of MCP-1 and IL-6. After a shorter incubation of 6 hrs with IL-1β, MCP-1 secretion by human astrocytes was clearly detectable and significantly reduced in the presence of 2500 nM IRAK inh (Figure 5B).

For comparison, the effect of 2500 nM IRAK inh was also tested on other cell types, U373 and primary adult human microglia. Incubation of human astrocytoma U373 cells with 10 U/ml IL-1β for 6 hrs clearly induced MCP-1 secretion (Figure 6A). Co-incubation with IRAK inh significantly reduced the IL-1β-induced secretion MCP-1 by U373 cells, an effect comparable to that observed with human primary astrocytes (Figure 6B). Next the effect of IRAK inh was assessed on the proinflammatory response in human primary microglia elicited by lipopolysaccharide (LPS). Whereas a marked increase in MCP-1 secretion levels was observed after 6 hrs incubation with LPS (Figure 6C), co-incubation with IRAK inh completely inhibited the secretion of MCP-1. This data indicates that IRAK inh is a potent inhibitor of proinflammatory cytokine secretion by human astrocytes and microglia.

IRAK1/4 inhibitor I does not reduce the uptake of Aβ by human primary astrocytes and microglia

Previously we have shown that human primary astrocytes and microglia can internalize Aβ1-42 [2,3]. In this study we have investigated whether IRAK inh affects the uptake of oligomeric or fibrillar preparations of Aβ1-42 (O-Aβ1-42 or F-Aβ1-42). Human primary astrocytes or microglia were incubated with O-Aβ1-42 or F-Aβ1-42 for 24 hours either with or without IRAK inh (2500 nM) after which the uptake was assessed by FACS analysis. As observed previously, human astrocytes internalize the smaller size O-Aβ1-42 more avidly than F-Aβ1-42 [24]. The uptake of either O-Aβ1-42 or F-Aβ1-42 by human astrocytes was not affected by IRAK inh. Similarly, the uptake of O-Aβ1-42 or F-Aβ1-42 by human primary microglia was not affected by IRAK inh after 24 hrs incubation (Figure 7). These data indicate that IRAK inh reduces a proinflammatory response elicited by human primary astrocytes and microglia without affecting the uptake of oligomeric or fibrillar preparations of Aβ1-42 by these cells.

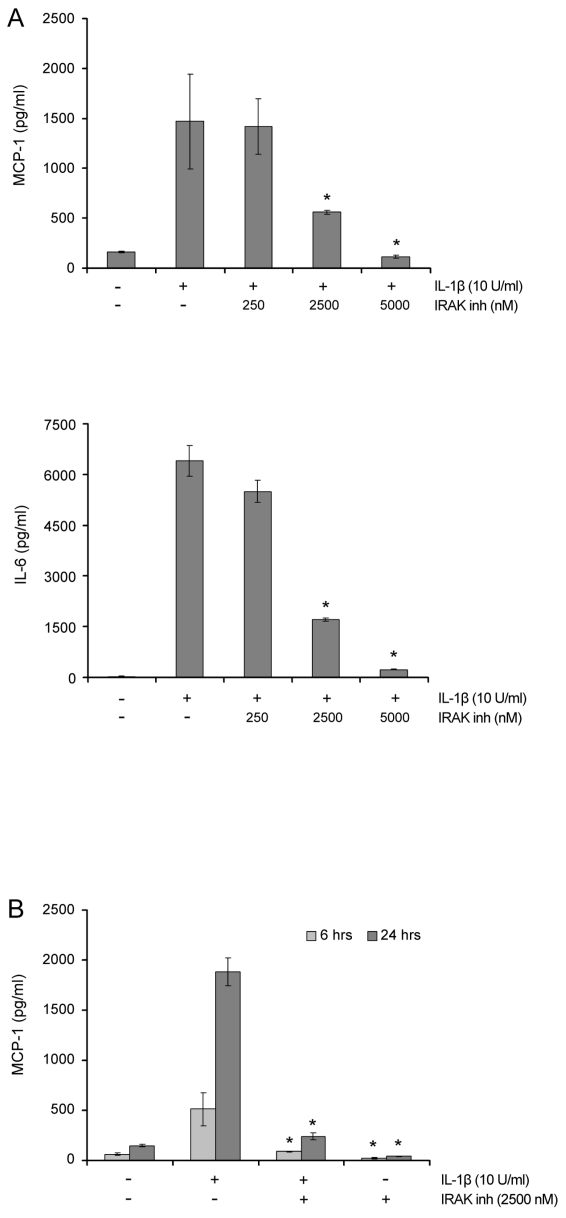

Figure 5: MCP-1 and IL-6 secretion by human primary astrocytes in the presence of IRAK-1/4 inhibitor I. **(A)** IL-1β (10 U/ml) induced secretion of MCP-1 (upper panel) and IL-6 (lower panel) after 24 hours detected in the supernatant of cultured human primary astrocytes in the presence of IRAK inhibitor I (250, 2500, and 5000 nM). **(B)** Effects of IRAK inhibitor I on the IL-1β (10 U/ml) induced secretion of MCP-1 as detected in the culture supernatant of human astrocytes after 6 and 24 hours incubation in the presence of 2500 nM IRAK inhibitor I. Results are expressed as mean (± SD) of one representative experiment assayed in triplicate. Asterisks indicate significant difference compared with IL-1β treatment without IRAK inhibitor I treatment ($p<0.05$).

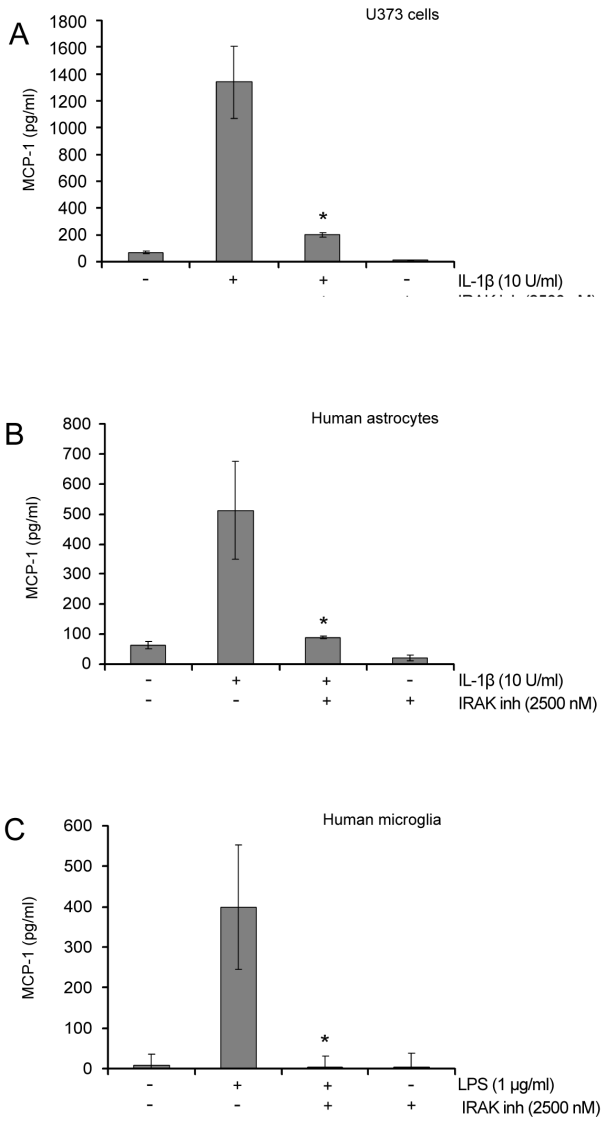

Figure 6: Effect of IRAK-1/4 inhibitor I on secreted MCP-1 levels in the culture supernatants of U373 cells, human astrocytes and human microglia after 6 hours incubation. **(A)** IL-1β (10 U/ml) induced MCP-1 secretion by U373 cells in the presence of IRAK inhibitor I (2500 nM). **(B)** IL-1β (10 U/ml) induced MCP-1 secretion by human primary astrocytes in the presence of IRAK inhibitor I (2500 nM). **(C)** LPS (1 μg/ml) induced MCP-1 secretion by human primary microglia in the presence of IRAK inhibitor I (2500 nM). Results are expressed as mean (± SD) of one representative experiment assayed in triplicate. Asterisks indicate significant difference compared with IL-1β or LPS treatment without IRAK inhibitor I treatment ($p < 0.05$).

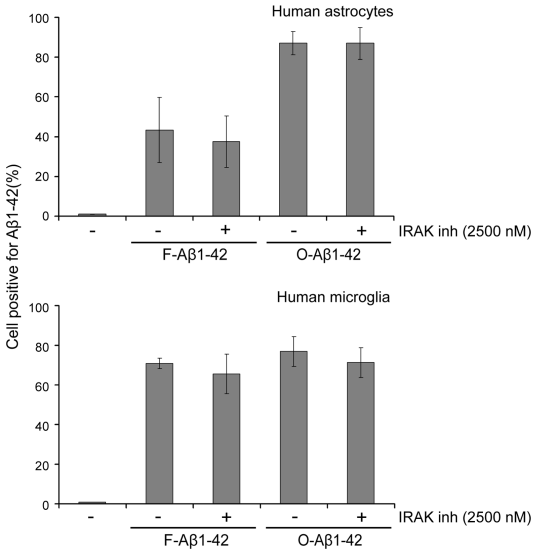

Figure 7: Uptake of Aβ1-42 by human primary astrocytes or microglia as measured by FACS in the presence of IRAK-1/4 inhibitor I. Cells that have internalized fluorescent labelled Aβ1-42 are expressed as percentage of the total number of cells counted using FACS (y-axis). Human astrocytes and human microglia were incubated for 24 hours with fluorescently labelled fibrillar Aβ1-42 (F-Aβ-1-42) or oligomeric Aβ1-42 (O-Aβ1-42) with or without IRAK inhibitor I (2500 nM). Results are expressed as mean (± SD) of three separate experiments.

Discussion

In this study we show that IRAK-4 protein kinase activity is increased in human AD temporal cortex compared with temporal cortex derived from non-neurological control cases. Previously, Cameron and colleagues reported that loss of IRAK-4 kinase activity results in decreased Aβ levels in an AD transgenic mouse model [19]. Accumulating evidence points towards functional differences in the IRAK signalling pathway between mouse and human [11], underscoring the importance of confirmation of these previous findings in human brain tissue and cells. In human brain tissue we were able to detect IRAK-4 in microglia and astrocytes. Cell culture experiments with human adult astrocytes and primary microglia show a potent decrease in respectively IL-1β- and LPS-induced MCP-1/IL-6 secretion in the presence of a small compound that selectively inhibits IRAK-1/4 kinase activity. In contrast, the uptake of Aβ oligomers or fibrils by human astrocytes and primary microglia remained unaffected in the presence of IRAK-1/4 inhibitor.

We have recently developed a new technique to determine and analyse protein kinase activity profiles in post-mortem brain tissue [5]. Here we compared peptides that are differently phosphorylated between CTRL and AD samples with existing STK profiles derived from human recombinant STKs. Comparing STK profiles of CTRL and AD samples with human recombinant STKs pointed towards an increased activity of IRAK-4 in AD. Although the micro array data suggest a prominent involvement of IRAK-4 kinase activity in AD brain, additional validation is imperative. Using immunohistochemistry we found significant increased levels of IRAK-4 in brain tissue derived from AD cases compared with control cases. Cui and colleagues previously reported that the levels of IRAK-4 in the superior temporal lobe remained un-altered between control and AD subjects while IRAK-1 levels were decreased in AD [27]. These discrepancies could be explained by the use of different detection techniques. The conclusions by Cui and colleagues are based on Western blot analysis of total protein lysates, while we have analysed specifically the grey matter of the temporal cortex by immunohistochemistry. Although we observed no significant difference in IRAK-1, the levels of phosphorylated (Ser376) IRAK-1 were found to be increased over 3-fold in AD compared with control cases. Increased IRAK-4 activity as indicated by elevated levels of pIRAK-1 in AD brain is supported by the increased protein kinase activity profile of IRAK-4 observed in AD brain tissue. Using double-immunofluorescence IRAK-4 could be observed in astrocytes and microglia. The prominent presence of IRAK-4 in microglia and astrocytes is in line with previous observations showing increased numbers of microglia and astrocytes in AD pathology [28,29].

IRAK-4 is a component of the signal transduction pathway that functions downstream TLRs. Within the context of neuroinflammation the TLR-mediated microglial response has beneficial roles in stimulating phagocytosis as well as detrimental roles in the release of neurotoxic products [17]. Increased expression of TLR4 in AD brain tissue is associated with amyloid plaque deposition [30]. Mouse microglia show increased ingestion of Aβ after activation of TLR4 *in vitro* [15]. MyD88 deficiency (MyD88(-/-)) in a transgenic AD mouse model (APPswe/PS1) decreases Aβ load as well as microglial activation in the brain [18]. Like IRAK signalling, the adapter protein MyD88 is essential for the downstream signalling of TLR4 leading to NF-κB activation [8]. Data from these reports and the results presented in this study indicate that selective inhibition of this pathway reduces the detrimental TLR-mediated microglial release of neurotoxic products without affecting the phagocytosis of Aβ. The possibility that small compounds that selectively inhibit kinase activity can be employed for this selective inhibition prospers hope for the development of new therapeutic drugs.

We show that the TLR/IL-1RI mediated secretion of MCP-1 by human microglia and astrocytes can be inhibited by an IRAK-1/4 inhibitor. The small inducible cytokine MCP-1 is under control of NF-κB and plays a prominent role in the inflammatory response in AD brain [31]. MCP-1 (also referred to as chemokine (C-C motif) ligand 2 (CCL2)) is consistently upregulated in AD brain tissue [31] and MCP-1 overexpression in an AD mouse model accelerates Aβ deposition by reducing Aβ clearance [32]. Interestingly, it has been suggested that an increased MCP-1 level in CSF is associated with a faster rate of cognitive decline during early stages of AD in humans [33].

New insight regarding the molecular regulation of inflammation in AD is warranted to understand the role of inflammation in AD and to use it as a therapeutic target. Epidemiological studies have indicated that systemic use of anti-inflammatory drugs can prevent or delay the development of AD [34,35]. However, clinical trials investigating the effects of anti-inflammatory drugs have failed or yielded inconclusive results [36]. The failure of these trials indicates that it is still unclear how different inflammatory components interact or at what stages of AD inflammation is beneficial or detrimental [37,38]. New insight regarding the molecular regulation of inflammation in AD is

warranted to understand the role of inflammation in AD and to use it as a therapeutic target. In this study we show support for increased IRAK-4 kinase activity in AD brain compared to non-demented control brain. The secretion of pro-inflammatory cytokines MCP-1 and IL-6 by human microglia and astrocytes can be selectively inhibited by IRAK-1/4 inhibitor I while uptake of Aβ by astrocytes and microglia is not affected. These results point towards the IRAK signalling pathway as a potential therapeutic target for modulating neuroinflammation in AD. Since the beneficial function of clearing Aβ is not affected, inhibition of the IRAK-4 signalling pathway merits further investigation.

Acknowledgement

This work was supported by a grant from the Alzheimer's Association (NIRG-12-241286). Human brain tissue was obtained from the Netherlands Brain Bank.

References

1. Akiyama H, Barger S, Barnum S, Bradt B, Bauer J, et al. (2000) Inflammation and Alzheimer's disease. See comment in PubMed Commons below Neurobiol Aging 21: 383-421.
2. Familian A, Eikelenboom P, Veerhuis R (2007) Minocycline does not affect amyloid beta phagocytosis by human microglial cells. See comment in PubMed Commons below Neurosci Lett 416: 87-91.
3. Nielsen HM, Veerhuis R, Holmqvist B, Janciauskiene S (2009) Binding and uptake of A beta1-42 by primary human astrocytes in vitro. See comment in PubMed Commons below Glia 57: 978-988.
4. Eikelenboom P, van Exel E, Veerhuis R, Rozemuller AJ, van Gool WA, et al. (2012) Innate immunity and the etiology of late-onset Alzheimer's disease. See comment in PubMed Commons below Neurodegener Dis 10: 271-273.
5. Hoozemans JJ, Hilhorst R, Ruijtenbeek R, Rozemuller AJ, van der Vies SM (2012) Protein kinase activity profiling of postmortem human brain tissue. See comment in PubMed Commons below Neurodegener Dis 10: 46-48.
6. Sikkema AH, Diks SH, den Dunnen WF, ter Elst A, Scherpen FJ, et al. (2009) Kinome profiling in pediatric brain tumors as a new approach for target discovery. See comment in PubMed Commons below Cancer Res 69: 5987-5995.
7. Ter Elst A, Diks SH, Kampen KR, Hoogerbrugge PM, Ruijtenbeek R, et al. (2011) Identification of new possible targets for leukemia treatment by kinase activity profiling. See comment in PubMed Commons below Leuk Lymphoma 52: 122-130.
8. Suzuki N, Saito T (2006) IRAK-4--a shared NF-kappaB activator in innate and acquired immunity. See comment in PubMed Commons below Trends Immunol 27: 566-572.
9. Wesche H, Henzel WJ, Shillinglaw W, Li S, Cao Z (1997) MyD88: An adapter that recruits IRAK to the IL-1 receptor complex. Immunity 7: 837-847.
10. Burns K, Martinon F, Esslinger C, Pahl H, Schneider P, et al. (1998) MyD88, an adapter protein involved in interleukin-1 signaling. See comment in PubMed Commons below J Biol Chem 273: 12203-12209.
11. Flannery S, Bowie AG (2010) The interleukin-1 receptor-associated kinases: critical regulators of innate immune signalling. See comment in PubMed Commons below Biochem Pharmacol 80: 1981-1991.
12. Griffin WS, Sheng JG, Roberts GW, Mrak RE (1995) Interleukin-1 expression in different plaque types in Alzheimer's disease: significance in plaque evolution. See comment in PubMed Commons below J Neuropathol Exp Neurol 54: 276-281.
13. Shaftel SS, Griffin WS, O'Banion MK (2008) The role of interleukin-1 in neuroinflammation and Alzheimer disease: an evolving perspective. See comment in PubMed Commons below J Neuroinflammation 5: 7.
14. Fassbender K, Walter S, Kühl S, Landmann R, Ishii K, et al. (2004) The LPS receptor (CD14) links innate immunity with Alzheimer's disease. See comment in PubMed Commons below FASEB J 18: 203-205.
15. Tahara K, Kim HD, Jin JJ, Maxwell JA, Li L, et al. (2006) Role of toll-like receptor signalling in Abeta uptake and clearance. See comment in PubMed Commons below Brain 129: 3006-3019.
16. Udan ML, Ajit D, Crouse NR, Nichols MR (2008) Toll-like receptors 2 and 4 mediate Abeta(1-42) activation of the innate immune response in a human monocytic cell line. See comment in PubMed Commons below J Neurochem 104: 524-533.
17. Landreth GE, Reed-Geaghan EG (2009) Toll-like receptors in Alzheimer's disease. See comment in PubMed Commons below Curr Top Microbiol Immunol 336: 137-153.
18. Lim JE, Kou J, Song M, Pattanayak A, Jin J, et al. (2011) MyD88 deficiency ameliorates Î²-amyloidosis in an animal model of Alzheimer's disease. See comment in PubMed Commons below Am J Pathol 179: 1095-1103.
19. Cameron B, Tse W, Lamb R, Li X, Lamb BT, et al. (2012) Loss of interleukin receptor-associated kinase 4 signaling suppresses amyloid pathology and alters microglial phenotype in a mouse model of Alzheimer's disease. See comment in PubMed Commons below J Neurosci 32: 15112-15123.
20. Braak H, Braak E (1991) Neuropathological stageing of Alzheimer-related changes. See comment in PubMed Commons below Acta Neuropathol 82: 239-259.
21. de Groot CJ, Hulshof S, Hoozemans JJ, Veerhuis R (2001) Establishment of microglial cell cultures derived from postmortem human adult brain tissue: immunophenotypical and functional characterization. See comment in PubMed Commons below Microsc Res Tech 54: 34-39.
22. Hoozemans JJ, Veerhuis R, Janssen I, van Elk EJ, Rozemuller AJ, et al. (2002) The role of cyclo-oxygenase 1 and 2 activity in prostaglandin E(2) secretion by cultured human adult microglia: implications for Alzheimer's disease. See comment in PubMed Commons below Brain Res 951: 218-226.
23. Alley MC, Scudiero DA, Monks A, Hursey ML, Czerwinski MJ, et al. (1988) Feasibility of drug screening with panels of human tumor cell lines using a microculture tetrazolium assay. See comment in PubMed Commons below Cancer Res 48: 589-601.
24. Nielsen HM, Mulder SD, Beliën JA, Musters RJ, Eikelenboom P, et al. (2010) Astrocytic A beta 1-42 uptake is determined by A beta-aggregation state and the presence of amyloid-associated proteins. See comment in PubMed Commons below Glia 58: 1235-1246.
25. Chafekar SM, Hoozemans JJ, Zwart R, Baas F, Scheper W (2007) Abeta 1-42 induces mild endoplasmic reticulum stress in an aggregation state-dependent manner. See comment in PubMed Commons below Antioxid Redox Signal 9: 2245-2254.
26. Powers JP, Li S, Jaen JC, Liu J, Walker NP, et al. (2006) Discovery and initial SAR of inhibitors of interleukin-1 receptor-associated kinase-4. See comment in PubMed Commons below Bioorg Med Chem Lett 16: 2842-2845.
27. Cui JG, Li YY, Zhao Y, Bhattacharjee S, Lukiw WJ (2010) Differential regulation of interleukin-1 receptor-associated kinase-1 (IRAK-1) and IRAK-2 by microRNA-146a and NF-kappaB in stressed human astroglial cells and in Alzheimer disease. See comment in PubMed Commons below J Biol Chem 285: 38951-38960.
28. Arends YM, Duyckaerts C, Rozemuller JM, Eikelenboom P, Hauw JJ (2000) Microglia, amyloid and dementia in alzheimer disease. A correlative study. See comment in PubMed Commons below Neurobiol Aging 21: 39-47.
29. Hoozemans JJ, van Haastert ES, Veerhuis R, Arendt T, Scheper W, et al. (2005) Maximal COX-2 and ppRb expression in neurons occurs during early Braak stages prior to the maximal activation of astrocytes and microglia in Alzheimer's disease. See comment in PubMed Commons below J Neuroinflammation 2: 27.
30. Walter S, Letiembre M, Liu Y, Heine H, Penke B, et al. (2007) Role of the toll-like receptor 4 in neuroinflammation in Alzheimer's disease. See

comment in PubMed Commons below Cell Physiol Biochem 20: 947-956.

31. Sokolova A, Hill MD, Rahimi F, Warden LA, Halliday GM, et al. (2009) Monocyte chemoattractant protein-1 plays a dominant role in the chronic inflammation observed in Alzheimer's disease. See comment in PubMed Commons below Brain Pathol 19: 392-398.
32. Yamamoto M, Horiba M, Buescher JL, Huang D, Gendelman HE, et al. (2005) Overexpression of Monocyte Chemotactic Protein-1/CCL2 in ß-Amyloid Precursor Protein Transgenic Mice Show Accelerated Diffuse ß-Amyloid Deposition. Am J Pathol 166: 1475-1485
33. Westin K, Buchhave P, Nielsen H, Minthon L, Janciauskiene S, et al. (2012) CCL2 is associated with a faster rate of cognitive decline during early stages of Alzheimer's disease. See comment in PubMed Commons below PLoS One 7: e30525.
34. in t' Veld BA, Ruitenberg A, Hofman A, Launer LJ, van Duijn CM, et al. (2001) Nonsteroidal antiinflammatory drugs and the risk of Alzheimer's disease. See comment in PubMed Commons below N Engl J Med 345: 1515-1521.
35. McGeer PL, Schulzer M, McGeer EG (1996) Arthritis and anti-inflammatory agents as possible protective factors for Alzheimer's disease: a review of 17 epidemiologic studies. See comment in PubMed Commons below Neurology 47: 425-432.
36. van Gool WA, Aisen PS, Eikelenboom P (2003) Anti-inflammatory therapy in Alzheimer's disease: is hope still alive? See comment in PubMed Commons below J Neurol 250: 788-792.
37. Breitner JC, Baker LD, Montine TJ, Meinert CL, Lyketsos CG, et al. (2011) Extended results of the Alzheimer's disease anti-inflammatory prevention trial. See comment in PubMed Commons below Alzheimers Dement 7: 402-411.
38. Hoozemans JJ, Veerhuis R, Rozemuller JM, Eikelenboom P (2011) Soothing the inflamed brain: effect of non-steroidal anti-inflammatory drugs on Alzheimer's disease pathology. See comment in PubMed Commons below CNS Neurol Disord Drug Targets 10: 57-67.

This article was originally published in a special issue, entitled: **"Neuroinflammatory Diseases",** Edited by Dr. David J Vigerust, Vanderbilt University School of Medicine, USA